Materials Research Proceedings 41 (2024) 1705-1713 https://doi.org/10.21741/9781644903131-189

Dissimilar welding of aluminum to AlSi-coated steel sheets using refill friction stir spot welding: A feasibility study

SHEN Tong[1,a *], FU Banglong[1,b], CHEN Ting[1,c], SUHUDDIN Uceu[1,d] and KLUSEMANN Benjamin[1,2,e]

[1]Helmholtz-Zentrum Hereon, Institute of Material Mechanics, Solid State Materials Processing, Max-Planck-Str. 1, Geesthacht 21502, Germany

[2] Leuphana University Lüneburg, Institute for Production Technology and Systems, Universitätsallee 1, Lüneburg 21335, Germany

[a]tong.shen@hereon.de, [b]banglong.fu@hereon.de, [c]ting.chen@hereon.de, [d]uceu.suhuddin@hereon.de, [e]benjamin.klusemann@hereon.de

Keywords: Refill Friction Stir Spot Welding, Aluminum, Steel, Dissimilar Materials Joining Lap-Shear Properties

Abstract. The main objective of this study was to assess and enhance the weldability of AA6016-T4 to AlSi-coated press-hardened steel (PHS), with a focus on investigating the impact of the AlSi coating on the mechanical properties of welded joints. Variations in tool rotation speed, dwell time, and plunge speed were performed to observe their effects on the joint behavior. It was observed that the protective AlSi-coating significantly influences the mechanical strength of the welded joint. Notably, the removal of the AlSi coating resulted in a substantial increase in joint mechanical strength. To systematically assess joint lap-shear strength under static loading conditions, Design of Experiment technique was employed. The influence of the process parameters on joint strength was thoroughly evaluated.

Introduction

In response to the escalating threat of global warming and the imperative to reduce greenhouse gas emissions, the EU's 2030 climate and energy framework targets a substantial 55% reduction in emissions compared to 1990 levels [1]. To get on track with the goals in the 2030 scenario, light-weighting of vehicles has been adopted by both governments and automotive industries as one of the most promising approaches. Over the past two decades, the utilization of modern advanced high-strength steels (AHSS) and press-hardening steel (PHS) have allowed for thinner/lighter body-in-white (BiW) structures [2]. These steel structures can be further combined with aluminum (Al) cast nodes and extrusions to reduce the weight effectively without compromising the costs, safety, and performance.

Although welding techniques for Al/steel dissimilar material joints have been developed to address problems in mechanical fastening and adhesive bonding, the application of the welding processes to join steel to aluminum is still difficult. The thermophysical properties of Al and iron (Fe) [3,4] show great differences in melting/boiling points, thermal expansion coefficient, thermal conductivity, specific heat, etc., as a result, defects as cracks, porosities, distortions occur in conventional fusion welding methods. Most importantly, according to the Al-Fe equilibrium phase diagram [5], Al and Fe have limited mutual solubility, thus hard and brittle intermetallic compounds (IMCs) form easily, which decrease the performance of the joint severely. According to the measured properties of Fe-Al IMCs [6], the Fe-rich IMCs (Fe_3Al, FeAl) show much lower hardness than the Al-rich IMCs (Fe_2Al_7, $FeAl_2$, Fe_2Al_5, and $FeAl_3$), which are preferable in Al/steel dissimilar welding. However, based on the thermodynamic calculations [7], Al-rich IMCs, especially the Fe_2Al_5, are more prone to form due to the lower reaction enthalpy. Moreover, the

crystal structure of Fe_2Al_5 is characterized with 30% vacancies along the c-axis [8], it grows rapidly and irregularly, which will decrease the performance of the joint. Several attempts have been conducted to control the heat input in fusion welding methods to reduce the formation of Al-rich IMCs and then improve the strength, which include cold metal transfer [9], implementation of high-power beams like electron beam [10] and laser beam [11], as well as laser-arc hybrid source [12]. The brazing-fusion welding method, i.e. the Al and filler metals (if used) melt while the steel is kept in solid state, can regulate the IMCs effectively. For instance, in laser brazing-fusion welding with Al-Si-Zn filler wire [13], the thickness of Fe-Al IMCs was suppressed below 10 μm due to the absence of melting of steel, and at the same time, the brittleness of the IMCs was decreased with the formation of Fe-Al-Si-Zn IMCs, leading to an improved mechanical strength of the weld.

As a solid-state welding process, friction stir welding (FSW) can eliminate the common problems in fusion welding due to the absence of melting and solidification. Additionally, a thin IMC layer can be produced with low heat input during FSW of Al/Ti [14]. These advantages have benefited its successful industrial production for Al/steel dissimilar components [15], where, compared to conventional welding, FSWed joints showed increased strength, absence of distortion, elimination of environmental pollution, higher space saving with reduced energy consumption by 50 %. Currently, it is estimated that around 85 % of the welding work in the automotive industry is related to spot welds [16] . Thus, the modified spot welding method based on FSW, friction stir spot welding (FSSW), was developed. Although Al/steel spot welds can be produced by FSSW [17] , an exit hole is left on the surface of the joint, resulting in problems such as decreased mechanical properties, potential stress concentration preferred sites for corrosion, etc.

As a solution, the refill friction stir spot welding (refill FSSW), a solid-state spot welding process to produce joints without an exit hole, was developed [18]. Refill FSSW is characterized by high energy efficiency and does not require additional filler materials, shielding gases for the operation, etc. The refill FSSW process has two variants depending on the plunge component into the material: probe plunge (PP) and shoulder plunge (SP) variant. The shoulder has a larger tip and side surfaces than the probe, so the SP variant can introduce a higher heat input and produce a larger joint than the PP variant. This results in more efficient material stirring and leads to a stronger joint. The SP variant is used in this study, it consists of four stages, as schematically illustrated in Fig. 1.

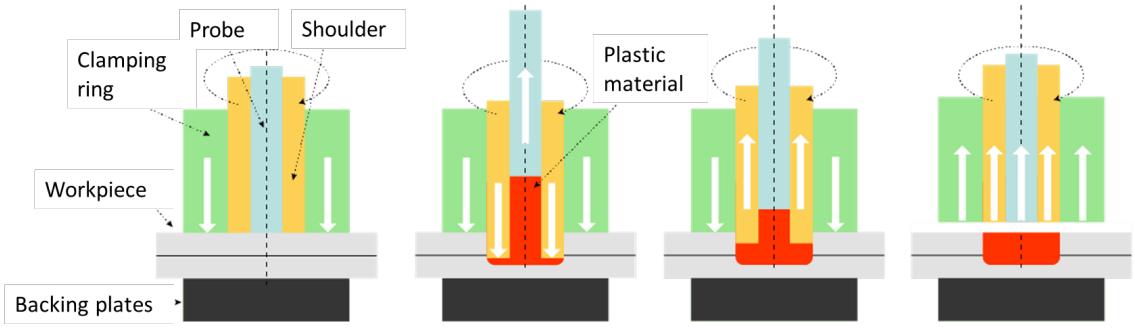

Fig. 1 Schematic illustration of SP variant of refill FSSW process

When applying refill FSSW to Al/press-hardened steel (PHS) with AlSi-coating, Ding et al. [19] analyzed the failure behavior and found that, the cracks mainly propagated through the AlSi-coating and AlSi/Al-Fe-Si interface. To enhance the understanding of the impact of AlSi coating on the weldability of Al/PHS steel joining, the current study conducts a direct comparison of the mechanical behavior of joints with varying PHS surface conditions. Furthermore, this study also

presents the significance of refill FSSW parameters, namely rotational speed (RotSpeed), dwell time (DweTime), and plunge speed (PluSpeed), in relation to the weld strength of the resulting joint.

Material and Methods

The AlSi-coated steel sheets utilized in this study were AlSi-coated PHS1500 steel, having a thickness of 1.5 mm and an average AlSi coating mass of 80 g/m². The chemical composition is listed in Tab. 1. To compare the weld outcomes with and without the presence of AlSi coating on the steel, a diamond disk grinder is utilized to eliminate the coating layer. The aluminum plates used in this study were AA6016-T4 aluminum alloy with a thickness of 1.2 mm. Overlap single joints were carried out using a Harms & Wende® RPS100-v32 machine, employing a non-consumable welding tool with probe, shoulder, and clamping ring diameters of 6 mm, 9 mm, and 17 mm, respectively. The employed process parameters are given in the following section.

Tab. 1 Chemical composition of AlSi-coated PHS1500 steel (wt %)

Steel Grade	C	Si	Mn	P	S	Al	Cu	Cr	N	Ti+Nb	Cr+Mo	B
PHS1500	0.19 – 0.25	1.00 – 1.70	0.030	0.005	0.15 - 0.50	0.35	0.35	0.02 - 0.05	0.02 - 0.06	0.009	0.19 - 0.25	1.00 - 1.70

Standard metallographic procedures were applied using Struers Tegramin-30 equipment to investigate the polished cross-sections of the obtained joints. The macro- and microstructures of the joints were observed via a Keyence VHX-6000 optical microscope (OM) and a FEI Quanta 650 FEG scanning electron microscope (SEM), which was fitted with an energy-dispersive X-ray spectroscopy (EDS) and electron backscatter diffraction (EBSD) detector. Quasi-static lap shear tests were conducted using a Zwick/Roell 1478 universal testing machine with a consistent cross-head speed of 1 mm/min at ambient temperature. All testing samples were fabricated into coupons measuring 90 mm x 115 mm, according to the DIN EN ISO 14273 standard [20]. Design of Experiment is employed as a robust statistical tool commonly employed in the analysis and optimization of industrial processes. With the support of the statistical analysis software Minitab, the number of experiments necessary for each design method can be generated. It also enables the analysis of how the performance of the weld responds to variations in welding variables. In this work, a three-factor three-level Box-Behnken experimental Design (BBD) has been employed.

Results and Discussion

The PHS sheets employed in this study are coated with a consistent layer of AlSi, maintaining a thickness of 30 ± 2 μm. An ultra-thin layer of Fe-Al inter-metallic compound (IMC), measuring 9 ± 1 μm, is present between the AlSi coating and the steel matrix, as illustrated in Fig. 3(a). Fig. 4 illustrates the EDS concentration profiles across the coating layer to the steel substrate. The line scanning result revealed the presence of multiple sublayers distinguished by their chemical compositions and thicknesses. To assess the weldability of AlSi-coated PHS, the impact of different surface conditions on the mechanical properties of the joints is investigated. Two distinct surface conditions of PHS sheets were produced: 1) The original PHS sheet with the AlSi coating, without any additional surface treatment. 2) Mechanically grinding all the coating layers, exposing the PHS steel matrix, as shown in Fig. 3(b).

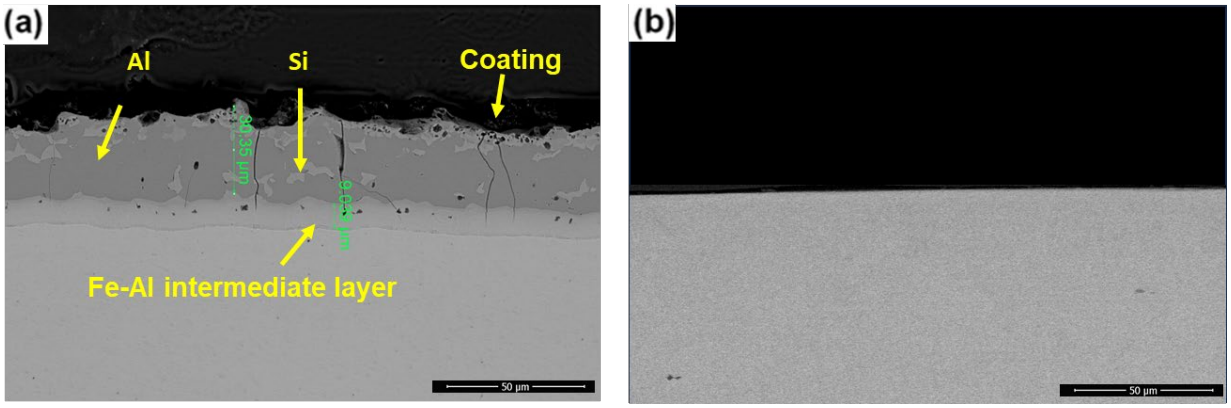

Fig. 3(a). Microstructure of a) AlSi-coated PHS steel (b) PHS steel after AlSi-coating removal

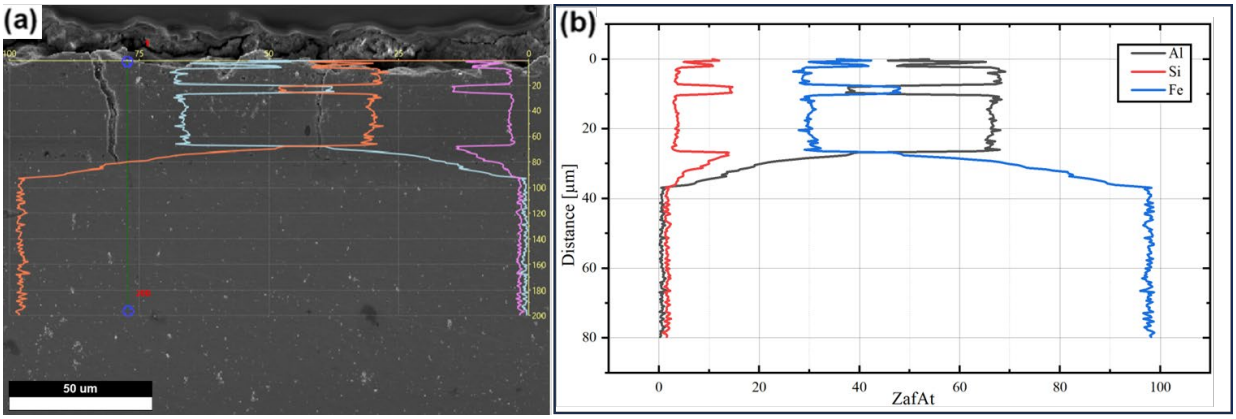

Fig. 4. EDS scanning results of AlSi-coating (a) coating layer of the as-received base material, (b) line scanning result shown in (a)

The AlSi-coated PHS sheets with varied surface conditions were then joined with AA6016-T4 sheets, using refill FSSW. A summary of the employed process parameters is presented in Tab. 2. The peeling off, i.e. absence of bonding, of welded joints has been observed and marked for the corresponding joint in Tab. 2. Six different parameter settings were employed for each surface condition to vary the heat inputs. For each surface condition, six samples were allocated for microstructure analysis, and an additional six samples were designated for weld strength measurements. The lap-shear strength (LSS) comparison for different surface conditions of PHS1500 is plotted in Fig. 5.

Tab. 2. Summarization of comparison study of different surface conditions of PHS sheets lap-shear strength of dissimilar AA6016-PHS1500 joints.

Weld No.	RotSpeed (rpm)	PluSpeed (mm/s)	DweTime (s)	LSS (N)	Surface condition
GT01.og	2400	1	0	1270	AlSi-coated PHS
GT02.og	2400	1	1	558	
GT03.og	2500	1	2	428	
GT04.og	2000	1	0	1370*	
GT05.og	1800	1	2	981	
GT06.og	1500	1	0	**	
GT01.C	2400	1	0	4650	Uncoated PHS
GT02.C	2400	1	1	5010	
GT03.C	2500	1	2	5190	
GT04.C	2000	1	0	4430	
GT05.C	1800	1	2	4920	
GT06.C	1500	1	0	5500	

*Indicates the absence of bonding in the sample.

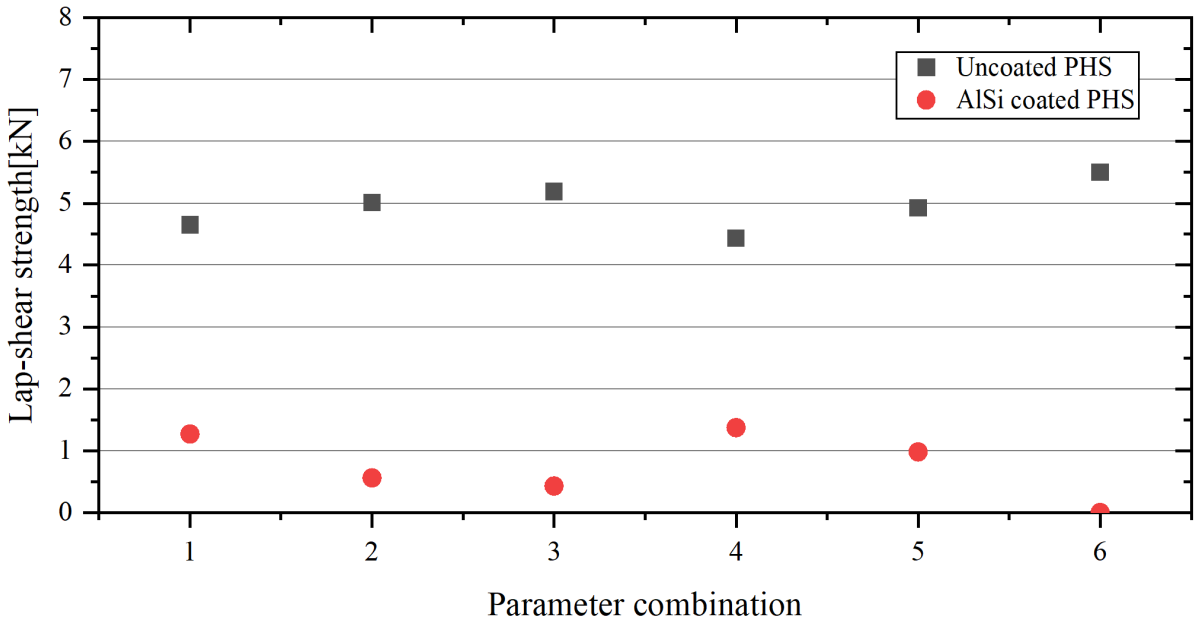

Fig. 5 Comparison of lap-shear strength for different surface conditions PHS1500 when joined with AA6016-T4

Results indicate that with the original AlSi coating, weak bonding or even unbonded areas are commonly observed. Upon removing the AlSi coating, the weld strength noticeably increases. The elimination of the coating layer results in a strength improvement of at least threefold. Cross-sectional macrostructures in Fig. 6 depict the typical appearance of the joining interface in the stirred zone (SZ) of samples with and without the coating layer. The macrograph depicting the joint without AlSi coating, as illustrated in Fig. 6(a), reveals an absence of welding defects. However, in the joint with AlSi coating, as depicted in Fig. 6(b), cracks are evident in the weld. Figure 6(a) further highlights the presence of cracks in the shoulder area, suggesting the

challenging establishment of metallurgical bonding between AlSi coating and Al. This hindrance in achieving metallurgical bonding between dissimilar metals during welding can accelerate the rupture of the welded joint under load.

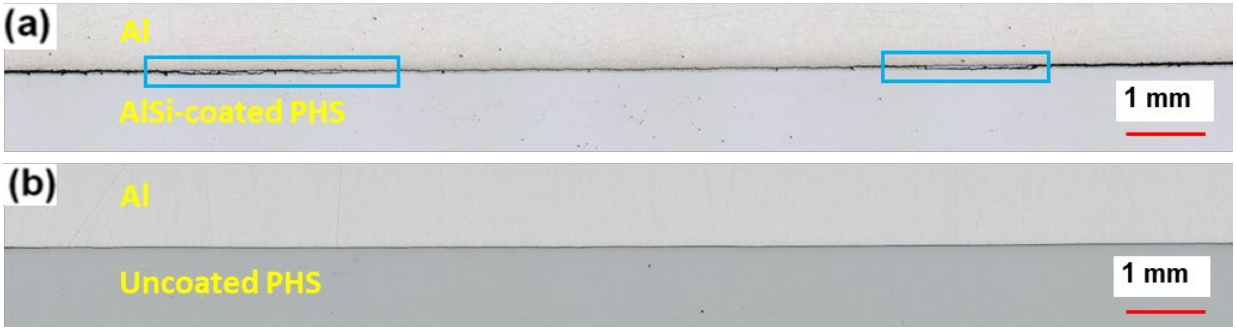

Fig. 6 Typical cross-sectional macrostructures of the joining interface in the stirred zone (SZ) of samples (a) with and (b) without the AlSi coating layer (RotSpeed: 2400 rpm, PluSpeed: 1 mm/s, DweTime 0 s, PluDepth 1.1 mm).

According to the defined parameter windows for dissimilar welding of AA6016 to PHS1500, a BBD was used for parameter optimization. The investigated parameters and the related levels in the BBD are summarized in Tab. 3. The removal of the AlSi coating from the PHS sheets is regarded as surface pre-treatment in the following.

Tab. 3 Investigated refill FSSW parameters and the related levels in the BBD for dissimilar welding of AA6016 to PHS1500. The AlSi coating has been removed from the PHS sheets.

Parameters	**-1**	**0**	**1**
Rotation speed (rpm)	1500	2000	2500
Dwell time (s)	0	1	2
Plunge speed (mm/s)	0.5	1	1.5

The normal probability plot, Fig. 7(a), confirms that the achieved LSS data fulfills the normality assumption. The Pareto chart obtained is shown in Fig. 7(b). According to the Pareto chart, the terms are arranged in descending order based on the decrease of their standardized effect on the mean LSS value. Rotational speed and dwell time are the only statistically significant parameters for the model. It is noteworthy that one of the main parameters, plunge speed, exhibits the least significance among all the terms in the model.

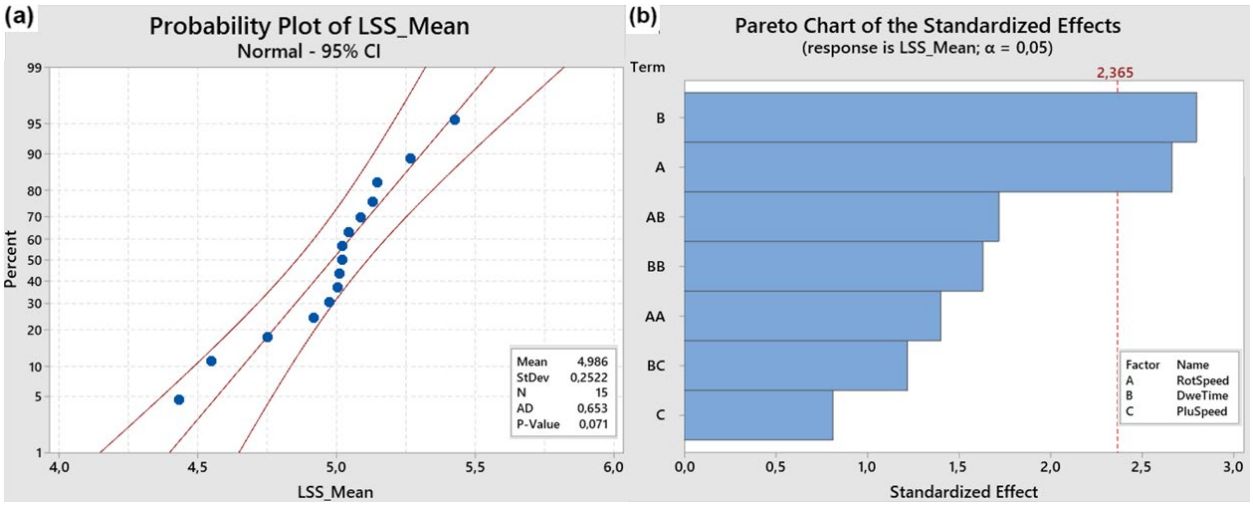

Fig. 7 (a) Normal probability plot of standardized residuals and (b) Pareto chart analysis of the main effects and interactions for LSS_Mean

The developed regression model was used to analyze the effects of welding parameters. Fig. 8(a) shows the main effects plot for the mean LSS. The effect of the most significant parameter rotational speed is confirmed by substantial variations in the mean value of LSS. The LSS decreases with the increase of rotational speed from 1500 to 2200 rpm and then exhibits an upward trend. Fig. 8(b) shows the interaction plot of combination of parameters on the LSS. The combination of rotational speed and dwell time, acknowledged as the most significant two-way interaction term, shows a strong influence on the LSS. When the rotational speed is higher than 2000 rpm, an increased dwell time is recommended to enhance the weld strength.

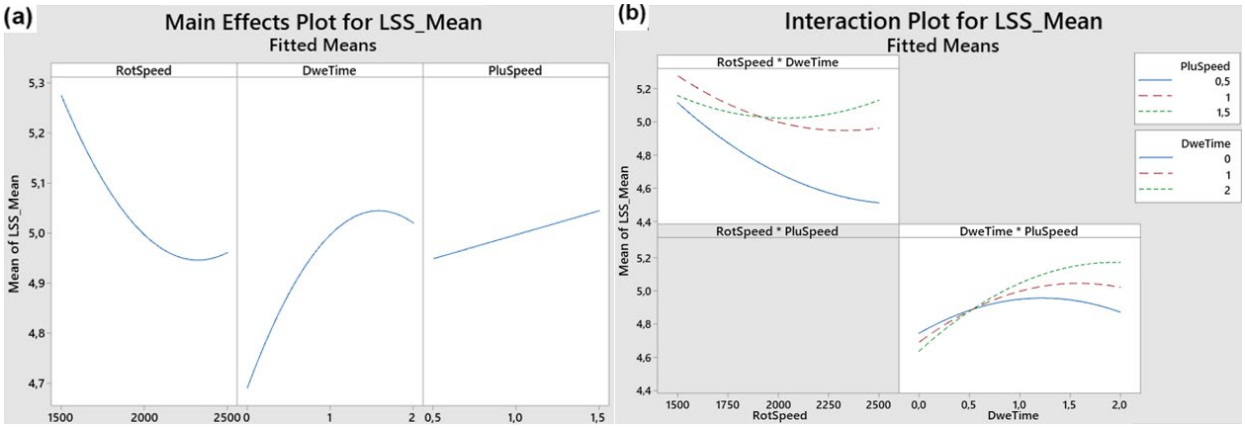

Fig. 8 (a) Main effect plots of the parameters on LSS, (b) Interaction plot of the parameters on LSS.

Summary

This preliminary study has effectively demonstrated the possibility to weld AA6016-T4 to AlSi-coated PHS1500 via refill FSSW. The impact of welding process parameters on the weld lap-shear strength of dissimilar joints was evaluated via statistical analysis. Based on the experimental results, the following conclusions can be drawn:

- The AlSi-coated PHS steel in its initial state exhibits a predominantly weak bond, with an average lap-shear strength of 0.9 kN.
- The elimination of the AlSi coating layer results in higher weld strength, averaging 4.95 kN. Significantly, each sample exhibits at least a threefold increase in strength compared to AlSi-coated surface conditions under identical welding conditions.

- Within the specified range of welding parameters, rotational speed proved to be the most influential parameter affecting the lap-shear strength of the joints, with the dwell time following as the next significant factor. Conversely, plunge speed exhibited no significant impact on the performance of the joints.

Acknowledgment
This result is part of the project titled "Friction stir welding for improving joinability of high-performance steels for automotive components to boost green road mobility — Stir4Steel". This project has received funding from the Research Fund for Coal and Steel under grant agreement No 101034068.

References

[1] COMMUNICATION FROM THE COMMISSION TO THE EUROPEAN PARLIAMENT. A Clean Planet for all A European strategic long-term vision for a prosperous, modern, competitive and climate neutral economy, 2018. https://eur-lex.europa.eu/legal-content/EN/TXT/?uri=CELEX:52018DC0773. Lesch, N. Kwiaton, F.B. Klose, Advanced High Strength Steels (AHSS) for Automotive Applications − Tailored Properties by Smart Microstructural Adjustments, Steel Res. Int. 88 (2017) 1700210. https://doi.org/10.1002/srin.201700210

[2] C. Lesch, N. Kwiaton, F.B. Klose, Advanced High Strength Steels (AHSS) for Automotive Applications − Tailored Properties by Smart Microstructural Adjustments, Steel Res. Int. 88 (2017) 1700210. https://doi.org/10.1002/srin.201700210

[3] A.S.M. International, ed., ASM Handbook Volume 1: Properties and Selection: Irons, Steels, and High-Performance Alloys, 10th edition, ASM International, Materials Park, Ohio, 1990.

[4] A.I.H. Committee, ASM Handbook Volume 2: Properties and Selection: Nonferrous Alloys and Special-purpose Materials, ASM International, 1990. https://books.google.de/books?id=wxA7AQAAIAAJ

[5] M.E. Schlesinger, E.M. Mueller, ASM Handbook, Volume 3: Alloy Phase Diagrams, ASM International, Materials Park, Ohio, 1983.

[6] L. Tricarico, R. Spina, D. Sorgente, et al., Effects of heat treatments on mechanical properties of Fe/Al explosion-welded structural transition joints, Mater. Des. 30 (2009) 2693–2700. https://doi.org/10.1016/j.matdes.2008.10.010

[7] R.W. Richards, R.D. Jones, P.D. Clements, et al., Metallurgy of continuous hot dip aluminizing, Int. Mater. Rev. 39 (1994) 191–212. https://doi.org/10.1179/imr.1994.39.5.191.

[8] J. Yang, J.P. Oliveira, Y. Li, et al., Laser techniques for dissimilar joining of aluminum alloys to steels: A critical review, J. Mater. Process. Technol. 301 (2022). https://doi.org/10.1016/j.jmatprotec.2021.117443

[9] J. Chen, B. Shalchi Amirkhiz, R. Zhang, et al., On the Joint Formation and Interfacial Microstructure of Cold Metal Transfer Cycle Step Braze Welding of Aluminum to Steel Butt Joint, Metall. Mater. Trans. A. 51 (2020) 5198–5212. https://doi.org/10.1007/s11661-020-05917-8

[10] G. Chen, J. Liu, X. Shu, et al., Beam scanning effect on properties optimization of thick-plate 2A12 aluminum alloy electron-beam welding joints, Mater. Sci. Eng. A. 744 (2019) 583–592. https://doi.org/10.1016/j.msea.2018.12.034

[11] M.J. Torkamany, S. Tahamtan, J. Sabbaghzadeh, Dissimilar welding of carbon steel to 5754 aluminum alloy by Nd:YAG pulsed laser, Mater. Des. 31 (2010) 458–465. https://doi.org/10.1016/j.matdes.2009.05.046

[12] G. Qin, Z. Lei, Y. Su, et al., Large spot laser assisted GMA brazing–fusion welding of aluminum alloy to galvanized steel, J. Mater. Process. Technol. 214 (2014) 2684–2692. https://doi.org/10.1016/j.jmatprotec.2014.06.011

[13] J. Yang, Z. Yu, Y. Li, et al., Influence of alloy elements on microstructure and mechanical properties of Al/steel dissimilar joint by laser welding/brazing, Weld. World. 62 (2018) 427–433. https://doi.org/10.1007/s40194-017-0540-z

[14] U. Dressler, G. Biallas, und U. Alfaro Mercado, „Friction stir welding of titanium alloy TiAl6V4 to aluminium alloy AA2024-T3“, Mater. Sci. Eng. A, Bd. 526, Nr. 1–2, S. 113–117, Nov. 2009. https://doi.org/10.1016/j.msea.2009.07.006

[15] Y. Kusuda, Honda develops robotized FSW technology to weld steel and aluminum and applied it to a mass-production vehicle, Ind. Robot Int. J. 40 (2013) 208–212. https://doi.org/10.1108/01439911311309889

[16] L. SELOVA, H. AYDIN, O. TUNCEL, et al., Mechanical Properties of Resistance Spot Welded Three-Sheet Stack Joints of Dissimilar Steels in Different Welding Time, (2019).

[17] T. Matsuda, K. Owada, A. Numata, et al., Influence of interfacial structure on the fracture behavior of friction stir spot welded dissimilar joints, Mater. Sci. Eng. A. 772 (2020) 138743. https://doi.org/10.1016/j.msea.2019.138743

[18] C. Schilling, J. dos Santos, Method and device for joining at least two adjoining work pieces by friction welding, (2004).

[19] Y. Ding, Z. Shen, A.P. Gerlich, Refill friction stir spot welding of dissimilar aluminum alloy and AlSi coated steel, J. Manuf. Process. 30 (2017) 353–360. https://doi.org/10.1016/j.jmapro.2017.10.006

[20] DIN EN ISO 14273, Specimen dimensions and procedure for tensile shear testing resistance spot, seam and embossed projection welds. In: DIN, the German Institute for Standardization, 2014.